AIAA JOURNAL
Vol. 43, No. 7, July 2005

Influence of Jet Inlet Conditions on Time-Average Behavior of Transverse Jets

Marina Campolo*
Universidad Complutense de Madrid, 28040 Madrid, Spain
Gian Maria Degano† and Alfredo Soldati‡
Università di Udine, 33100 Udine, Italy
and
Luca Cortelezzi§
McGill University, Montreal, Quebec H3A 2K6, Canada

Dynamics and dispersion mechanisms in transverse jets are partially controlled by jet-exit conditions that are intimately linked to the coupling between issuing jet and crossflow. Accurate knowledge of this coupling is crucial to plan repeatable and effective experiments, perform accurate computations, and design dispersion control devices. A simplified geometry is focused on, representing a plenum/nozzle and a wind/water tunnel, to characterize the time-averaged extent of the coupling between the jet and crossflow and its effect on jet penetration, with specific emphasis on the following: 1) The relative importance of simulating/neglecting the coupling between jet and crossflow within the nozzle/plenum (pipe) is established to reproduce the jet penetration observed experimentally. 2) The distance down the pipe is characterized to determine how far down the presence of the crossflow modifies the flow with respect to the case of a jet issuing in a quiescent fluid. 3) Variations calculated in jet penetration are quantified when different boundary conditions are used to simulate the jet. 4) The effect of different crossflow velocities at jet exit on simulated jet penetration is evaluated. Results discussed may provide a guideline for future computational investigations on transverse jets and a useful reference to understand the discrepancies observed between experimental and numerical results.

I. Introduction

MANY engineering applications (exhaust gas cooling, fuel injection in combustion chambers, spray coating, etc.) and environmental applications (chimney plumes, sewerage outfalls, agricultural spraying systems, etc.) rely on transverse jets to promote mixing between injectant and crossflow. In these applications, jet and crossflow merge, efficiently dispersing particles or droplets transported by the jet into the transverse stream. Experiments (for instance, Refs. 1 and 2) and numerical simulations[3–5] helped to identify the dominant, large-scale, vortical structures, namely, jet shear layer vortices, horseshoe vortices, counter-rotating vortex pairs (CVP), and wake vortices, characteristic of a transverse jet. These vortical structures, which have been extensively described by Fric and Roshko[1] and Kelso et al.,[2] among others, play a role in the dispersion process because they have sufficient spatial and temporal coherence to control the motion of inertial particles, determining their dispersion and preferential concentration.[6,7] Consequently, a detailed understanding of the flowfield dynamics is necessary to identify strategies to optimize and control the dispersion processes. An extended review of the material published on transverse jets is presented by Karagozian et al.[8]

In this context, the precise characterization of jet-exit conditions is a crucial starting point. Investigations of freejets[9–11] demonstrated that different jet-exit (nozzle) geometries (smooth contraction or long straight pipe) produce different mean velocities and turbulence profiles, in turn influencing the length of the jet potential core and the near-field mixing.[11] Similarly, studies on transverse jets[12,13] have shown that jet-exit conditions influence the near-field dynamics and mixing in the the near-field region. Unfortunately, the accurate characterization of the jet-exit conditions for transverse jets is much more complex than for freejets, from both an experimental and a numerical point of view. The flowfield is, in general, fully three-dimensional, and its development is intimately linked to the unsteady interaction between vorticity emanating from the pipe and vorticity from the crossflow boundary layer. In many experimental studies, this unsteady interaction is simply neglected, and the jet-flow characteristics are measured with the transverse flow turned off, that is, implicitly assuming that the jet flow at the exit plane and within the nozzle is not strongly influenced by the crossflow. This is not always the case, as we will show in this study. Similarly, crossflow characteristics, for example, the boundary-layer thickness, are measured with the jet turned off, that is, explicitly neglecting the strong nonlinear interaction between crossflow and jet.

Following Moussa et al.,[12] the uncertainty on the jet-exit conditions is one of the possible causes for the significant variations found in the literature for experimental results on jet rise. However, it is not yet clear which are the features of the jet velocity, the mean profile, the turbulence level, or the coupling with the crossflow, controlling the jet rise.

The uncertainty on the jet-exit conditions is also crucial when the jet is manipulated/controlled by means of jet velocity modulations. McCloskey et al.[14] have shown that accurate jet forcing can be achieved by dynamically compensating the nozzle/plenum. In other words, use of the compensation makes the jet forcing independent of the experimental apparatus.

Characterization of jet-exit conditions is also a sensitive point for numerical investigations. The crucial point is to determine 1) under

Received 2 April 2004; revision received 2 November 2004; accepted for publication 30 December 2004.

*Investigadora Postdoctoral, Instituto Pluridisciplinar; currently Technical Researcher, Centro Interdipartimentale di Fluidodinamica e Idraulica, Università de Udine, 33100 Udine, Italy.

†Student, Centro Interdipartimentale di Fluidodinamica e Idraulica; currently Employee, Danieli & C., Officine Meccaniche S.p.A., 33042 Buttrio (Udine), Italy.

‡Associate Professor and Head, Centro Interdipartimentale di Fluidodinamica e Idraulica, Dipartimento di Energetica e Macchine; soldati@uniud.it.

§Associate Professor, Department of Mechanical Engineering; currently Associate Professor, Dipartimento di Fisica, Università di Udine, 33100 Udine, Italy.

which conditions it is necessary to account for the coupling between jet and crossflow at the jet exit and 2) how this can be done in a cost-effective way. Most simulations are performed by imposing an analytical velocity profile and turbulence level at the jet exit,[15–17] or a time-dependent, fully developed pipe flow at some arbitrary distance inside the pipe/nozzle.[3] These approaches are not always able to reproduce precisely the mean velocity profile at the jet exit, which is reported by experiments to be not axisymmetric, with larger velocity values in the downstream region of the pipe.[13,18] Alternative approaches proposed in the literature account for the coupling in the plenum, imposing a constant total pressure at the jet exit.[19] These simulations reproduce precisely the mean velocity profile at the jet exit, and yet fail in reproducing the turbulence intensity level, which is crucial for mixing characterization.[19]

Despite the importance of establishing the role of jet-exit conditions for precise flowfield characterization of the transverse jet, to our knowledge, there is no work available in the literature in which 1) the importance of simulating the coupling between jet and crossflow is quantitatively assessed, 2) the extent of the coupling between jet and crossflow is quantified, and 3) modifications in jet penetration due to the choice of numerical boundary conditions are evaluated.

There are four aims of the present study: 1) We establish the relative importance of simulating/neglecting the coupling between jet and crossflow within the pipe (nozzle/plenum). 2) We characterize how far down the pipe the presence of the crossflow modifies the flow with respect to the case of a jet issuing in a quiescent fluid. 3) We quantify variations calculated in jet penetration when different boundary conditions are used for the jet. 4) We characterize the effect of the conditions found at the jet exit (different crossflow velocity and thickness of the unperturbed crossflow boundary layer) on the numerical simulation of the transverse jet.

II. Computational Methodology

Figure 1 shows the computational domain used in this study. The geometry of the domain is a simplification of the geometry of the test section of an experimental wind/water tunnel, with a pipe representing the plenum/nozzle system. The jet is issued by a long pipe perpendicular to the wind tunnel. The simplified geometry chosen allows us to obtain basic information on the coupling between jet and crossflow. On the one hand, the pipe is a convenient simplification of the large variety of plenum/nozzle geometries used in experiments. On the other hand, focusing our study on a given plenum/nozzle geometry would have been too restrictive.

The reference coordinate system is centered at the jet exit, with x, y, and z the streamwise, spanwise, and vertical directions, respectively. Jet and crossflow fluids are incompressible and, for simplicity, are assumed to be the same.

In our investigation, we consider only the time-averaged flow structure and jet-to-crossflow velocity ratios $\alpha = U_{\text{jet}}/U_{\text{cf}} \leq 20$, for which time-averaged velocity are available in literature.[20,21] The time-averaged approach is the usual framework chosen to analyze jet mixing characteristics. In experiments, unsteady effects are averaged out to correlate results with mean flow parameters, and measurements of fluid flow behavior are obtained averaging

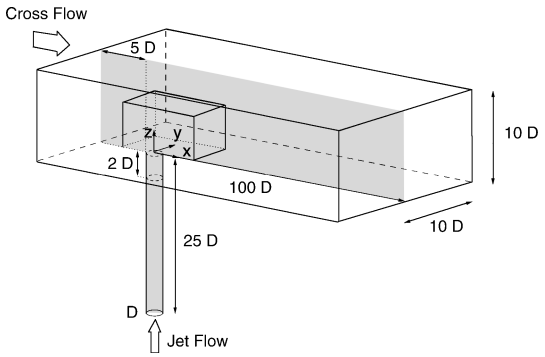

Fig. 1 Geometry of experimental apparatus with reference coordinate system.

over time samples collected discontinuously at different monitoring locations.

Experimental investigations[20,22] have shown that, in the range of parameters we investigate, unsteady phenomena do arise.[23] Specifically, helical-mode instabilities develop in the transverse jet, which break the symmetry of the CVP structure. Despite the simplifications involved in a time-average approximation, this analysis is a fundamental first step toward the full understanding of the coupling between jet and crossflow and may provide computational guidelines for future investigations.

Under the assumptions of time-averaged, symmetric flow structure, we solve for the flow over one-half of the domain only, as indicated by the shaded symmetry plane in Fig. 1. We implicitly assume that the time-averaged influence of asymmetric, helical modes are negligible with respect to the time-averaged influence of symmetric modes. Fully three-dimensional, time-dependent effects will be the object of future investigations.

The problem is made dimensionless using the orifice diameter D as a characteristic length and D/U_{jet} as a characteristic time. The test section is, thus, $106D$ long, $10D$ wide, and $10D$ high. The crossflow enters the domain $5D$ upstream of the jet orifice and the domain extends $100D$ downstream the jet orifice. The pipe is $25D$ long.

The computational domain is discretized into hexahedric finite volumes. A finer discretization is used for the jet-exit region, indicated by the smaller box in Fig. 1 ($-3 \leq x/D \leq 5, 0 \leq y/D \leq 4$, and $-3 \leq z/D \leq 4$), whereas the grid is hierarchically coarsened in the far field to capture the wide range of length scales characteristic of the flow.[20]

The fluid balance equations are solved in the Reynolds-averaged form using a commercial, finite volumes code (Star-CD®) and exploiting a standard k–ϵ model to reproduce the effects of the turbulent fluctuations. The k–ϵ model, with algebraic modeling of the wall layer (law of the wall), is simple and sufficiently accurate provided that the grid is accordingly refined near the boundaries, as in our study.

The solver uses two sets of variables, defining Cartesian velocities and pressure at cell centers, and contravariant volume fluxes at the cell faces. Flux discretization is obtained by a third-order (QUICK) scheme. The solution is obtained using the SIMPLE algorithm.[24] Momentum equations are solved by operator splitting using predictor/corrector stages. Equations for each dependent variable are decoupled and linearized and then solved using the conjugate gradient method. The pressure correction equation (Poisson equation) obtained from the continuity is solved using a multigrid algorithm.[25]

The boundary conditions for the numerical simulations are 1) uniform velocity profile of the crossflow at the inlet, 2) uniform velocity profile at the pipe inlet, 3) symmetry condition at the symmetry xz plane (Fig. 1), 4) zero-gradient outflow condition at the test-section outlet, and 5) no-slip conditions at all other boundaries. In agreement with previous experimental and numerical studies,[2,26] we impose at the pipe inlet and at the crossflow inlet the turbulent kinetic energy and the dissipation rate to be equal to 0.1 and to 0.001, respectively. Note that, because of the no-slip conditions, the pipe flow and crossflow develop their boundary layer at the walls of the computational domain.

Convergence to the steady-state solution is assessed by evaluating the value of the residuals of momentum and continuity equations as a function of the iteration number. We assumed that the computation has converged to the correct steady-state solution when the values of the residuals, normalized by the overall inflow (that is, jet plus crossflow) flow rate, are lower than 10^{-6}.

In our analysis, the object is to explore different jet-to-crossflow velocity ratios ($\alpha = 0.1$, 1., 2.2, 3, 4, 5, 6, 7, 9, 10, 14, and 20). Jet-to-crossflow velocity ratio and unperturbed crossflow boundary-layer thickness are two of the parameters controlling transverse jet behavior.[18] Therefore, we perform our simulations at different α 1) by changing the jet velocity only, so that in all cases we have the same unperturbed crossflow boundary-layer thickness at the jet exit, and 2) by changing the crossflow velocity only, to evaluate the effect of unperturbed boundary-layer thickness at the jet exit on jet development.

We validated our numerical experiment characterizing the sensitivity of our numerical solution in terms of grid resolution. Specifically, we considered two mesh models: MESH1, consisting of 630,152 finite volumes, and MESH2, consisting of 752,800 finite volumes. MESH2 was obtained by refining MESH1 in the jet-exit region ($-2 \le x/D \le 3$, $0 \le y/D \le 2$, and $-2 \le z/D \le 3$). Comparison between velocity isocontours calculated for MESH1 and MESH2 in the jet symmetry plane shows that differences are negligible. In fact, we found that the maximum variation of calculated velocity, scaled by the crossflow velocity, $\Delta u/U_{cf}$, is less than 0.18% in the last $2D$ of the pipe. This error can be made even smaller with further grid refinement, which was not possible with the presently available computational resources. Therefore, we chose the grid of 630,152 cells (57,600 for the pipe and 327,680 for the jet-exit region) to perform our analysis.

III. Results

A. Code Validation and Comparison with Shandorov Experiment

We validate our numerical methodology by replicating the experiment by Shandorov (see Ref. 21). The position of the jet axis is calculated from our simulation to establish a direct comparison with the experimental data by Shandorov and obtain a quantitative evaluation of the accuracy of our numerical approach.

In the experiment by Shandorov, an air jet with velocity $U_{jet} = 77.6$ m/s and a top-hat profile is injected from a nozzle with an orifice diameter $D = 0.02$ m into an air crossflow with velocity $U_{cf} = 35.6$ m/s. Note that the compressibility effects can be neglected for jet and crossflow velocities examined. The jet Reynolds number, $Re = U_{jet}D/\nu$, is $Re = 106{,}398$, and the jet-to-crossflow velocity ratio α is 2.2. Experimental data are available for the jet axis, which, in analogy with the freejet and as reported by Abramovich,[21] is defined as the locus of the points of maximum velocity.

In Fig. 2 the axis of the jet determined experimentally by Shandorov (solid line) is compared against the result of our computations (symbols). As reported by Abramovich,[21] the equation interpolating jet-axis data measured by Shandorov is given by

$$z/D = R^{0.79}(x/D)^{0.39} \tag{1}$$

In the coordinate system used, the center of the pipe is at $x/D = 0$, and the pipe wall is at $x/D = \pm 0.5$. In our computations, we calculate the jet behavior considering four different numerical boundary conditions that can be used to simulate the jet exit.

The first simulation (simulation A), identified by open triangles in Fig. 2, corresponds to a top-hat velocity profile imposed at the jet exit. This is the condition usually applied when a nozzle is used to issue the jet, as in Shandorov's experiment. It is implicitly assumed that the velocity profile is flat and that the coupling between jet and crossflow is negligible at the jet exit. Results are in good agreement with Shandorov's data up to $z/D < 1$, where the jet axis is coincident with the pipe/nozzle axis. Nevertheless, for $z/D > 1$, the jet axis is deflected less than in Shandorov's experiment.

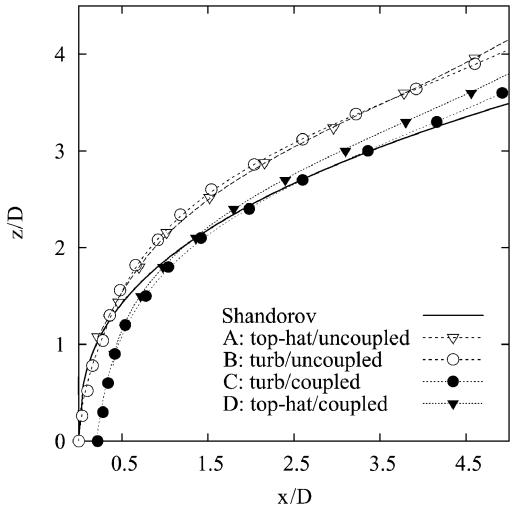

Fig. 2 Comparison between jet axis determined experimentally by Shandorov (solid line) and results of our numerical simulations (symbols).

As suggested by experiments and numerical simulations on freejets, the shape of the velocity profile imposed at the jet exit may play a role in jet calculation. Therefore, we performed a second simulation (simulation B), identified by open circles in Fig. 2, corresponding to fully developed turbulent jet flow imposed at the jet orifice. Results from this simulation show that differences in jet axis due to the different shapes of velocity profiles (simulations A and B) are small and do not explain the large difference with the experiment.

We performed two additional simulations to test the effect of the coupling between crossflow and jet. The third simulation (simulation C), identified by solid circles in Fig. 2, corresponds to a jet flow emerging from a $25D$-long pipe. The uniform velocity imposed at the pipe inlet becomes fully developed at about $15D$ from the pipe inlet, where velocity profile, kinetic energy profile, and dissipation profile compare well against our direct numerical simulation database.[27] At the jet orifice, the flow is turbulent and fully developed, and variations due to the coupling with the crossflow have been accounted for. Results are in excellent agreement with the experiment downstream the jet orifice. They differ from the experiment for $z/D < 2$, that is, in the region nearest the jet orifice, where the effect of the coupling between jet and crossflow is to move the jet-axis position downstream with respect to the prediction obtained from Shandorov data, as we will show in Sec. III.B.

We also evaluate whether the shape of the velocity profile affects the calculated jet axis. The fourth simulation (simulation D), identified by solid triangles in Fig. 2, corresponds to a jet flow emerging from a $2D$-long pipe. A top-hat velocity profile is imposed at the pipe inlet to account for the coupling between the jet and the crossflow. The agreement between numerical results and Shandorov data is, again, quite good, except in the region nearest the jet orifice, where the jet axis for a top-hat velocity profile is not well defined. In fact, multiple maxima exist near the jet exit. For this reason, the jet axis has been plotted only for $z/D > 1$ in Fig. 2.

From our results, it is clear that the choice whether or not to simulate the coupling between the jet and crossflow influences significantly the location of the jet axis at the jet exit and the jet development in the near field.[28] In the following section, the extent of this coupling and its effects on the jet penetration calculated numerically are further examined.

B. Quantification of Extent and Effects of Coupling Within the Pipe

To evaluate the extent of the coupling between the jet and crossflow within the pipe, we compare the velocity profile calculated inside the pipe when the transverse flow is on and when it is turned off, that is, as in the case of a freejet. We compare the results of the simulations performed when $\alpha = 2.2$, 4, and 7. In these simulations, the different values of α were obtained by fixing the crossflow velocity and changing only jet velocity, to have the same unperturbed crossflow boundary-layer thickness at the jet orifice.

Profiles shown in the top row of Fig. 3 correspond to the case when the transverse flow is on, whereas those in the central row correspond to the case when the transverse flow is turned off. The bottom row of Fig. 3 shows the comparison of the relative difference within the pipe between the axial velocity of the jet in crossflow, $w_{jcf}(r, \theta, z; \alpha)$, and the axial velocity of the freejet, $w_{fj}(r, \theta, z; \alpha)$. We show precisely the local velocity difference isosurfaces scaled by U_{jet}, that is, $(w_{jcf} - w_{fj})/U_{jet}$, calculated for $\alpha = 2.2$, 4, and 7 and the corresponding isocontours at $z/D = -1.0$, -0.5, and 0.0. Note that the structure of the isosurfaces is similar in all cases.

Let us first consider the local velocity difference isocontours calculated at the jet exit ($z/D = 0$) for $\alpha = 2.2$. The velocity of the jet reduces with respect to the freejet in the upstream region of the pipe and increases in the downstream region. The solid circle indicates the position of the maximum difference. This maximum difference is not on the symmetry plane, as one might expect; instead, it is near

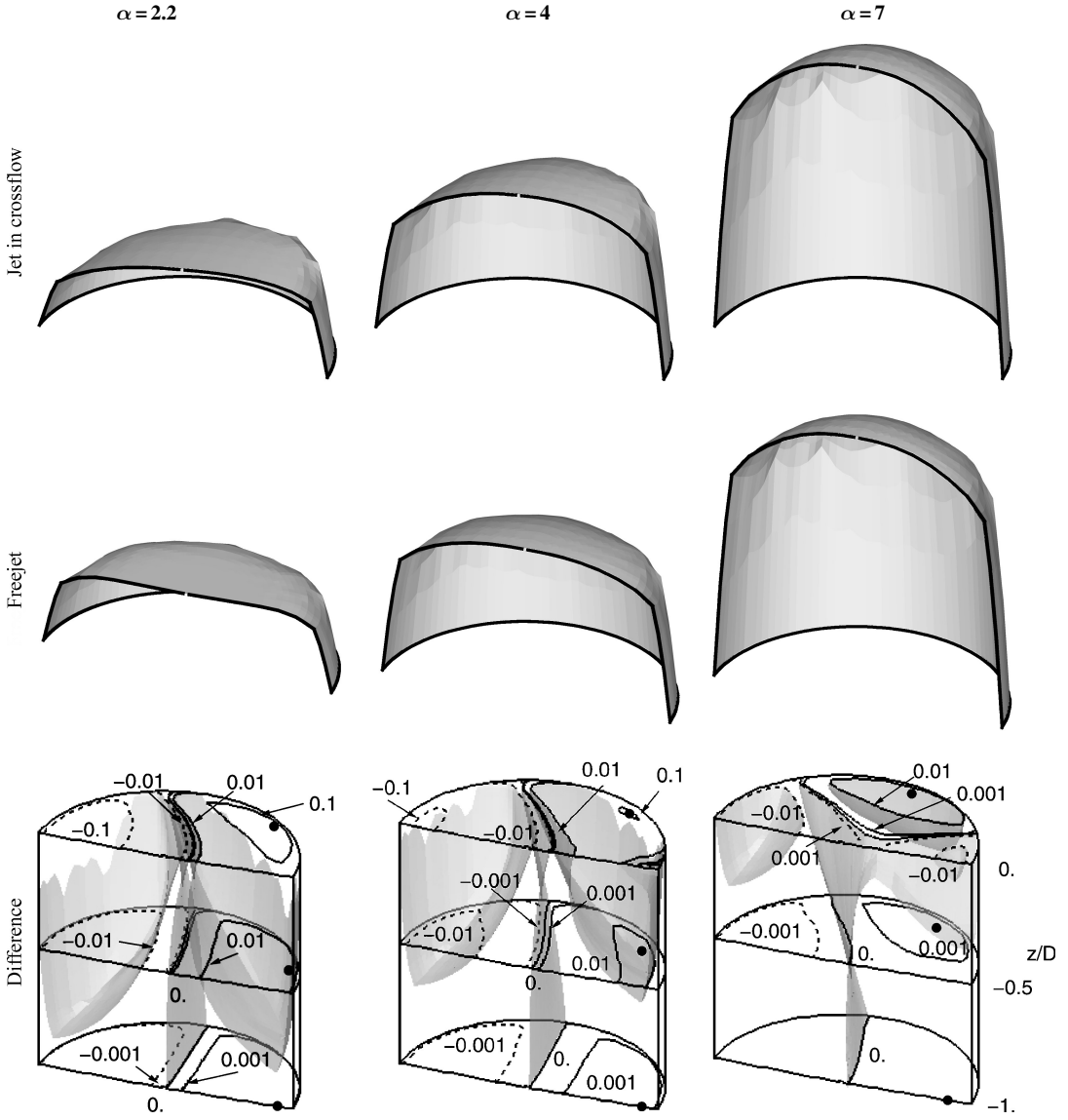

Fig. 3 Axial velocity profile at jet exit for jet in crossflow (top row), axial velocity profile at jet exit for free jet (central row), and isocontours of $(w - w_{\text{pipe}})/U_{\text{jet}}$ at $z/D = -1, -0.5$, and 0 for $\alpha = 2.2$, 4, and 7 (bottom row); ●, position of maximum velocity difference in cross section of pipe.

the pipe wall, in the downstream region of the pipe. We argue that this large deviation with respect to the freejet profile could be due to the presence of the CVP. In particular, the maximum difference could represent the footprint of the CVP.

Consider now local velocity difference isocontours calculated at the jet-exit section for values of α larger than 2.2. The values of the isocontours of the local velocity difference are smaller, and isocontours extend to reduced portions of the jet exit. The position of the maximum difference is still near the pipe wall and yet is progressively shifted less in the downstream direction. This seems to substantiate the hypothesis that the maximum difference could represent the footprint of the CVP. In fact, as α increases, the CVP tends to move toward to the side of the jet.

Consider, finally, the local velocity difference isocontours calculated deeper into the pipe. The isocontour values reduce for decreasing z/D, indicating that the profile of the pipe flow is progressively less affected by the crossflow as we move deeper inside the pipe. This effect is magnified as the value of α increases. Note that differences in the pipe flow due to the transverse stream are almost negligible for $\alpha = 7$.

These results are in qualitative agreement with previous experimental[13,2] and numerical investigations.[26] For instance, Andreopoulos and Rodi,[13] who focused only on the velocity profiles at the jet exit, report nonaxisymmetric axial velocity profiles and maximum axial velocity shifted progressively downstream the pipe center for decreasing α. Yet, to our knowledge, no quantitative investigation is available, and, furthermore, no investigations are available for the region inside the pipe near the jet exit.

We quantify how deep into the pipe the presence of the crossflow is felt by calculating the sectional relative difference (SRD) between the transverse jet and freejet as

$$\text{SRD}(z, \alpha) = \frac{1}{A} \int_A \frac{|w_{\text{jcf}} - w_{\text{fj}}|}{U_{\text{jet}}} \, \text{d}A \tag{2}$$

In Fig. 4 we show, for each α, the z_p at which $\text{SRD}(z_p, \alpha) = 0.001$. For clarity, a dotted cubic spline interpolant connects these points. Below this threshold, we assume that the coupling is negligible. As expected, for smaller α, the crossflow affects the flow deeper into the pipe. Note that $z_p(\alpha)$ varies almost linearly at intermediate values of α, $4 \le \alpha \le 7$ (solid line), whereas it saturates as α goes to zero and gradually approaches zero for $\alpha > 7$. Saturation for values of α smaller than four indicates that there is a maximum depth inside the pipe below which the external flow cannot affect the flow within the pipe. In the limiting case, when the jet flow is zero, the pipe behaves as a cavity, and the crossflow generates a series of recirculating cells of finite depth. This seems to be confirmed by a simulation performed when $\alpha = 0.1$. In this case, $z_p/D = -1.42$. This value

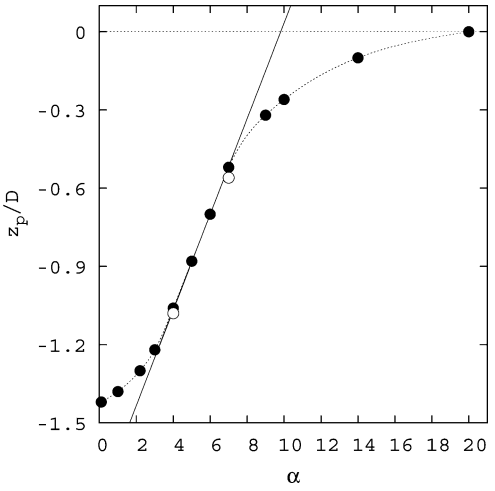

Fig. 4 Depth of crossflow interaction inside pipe for simulated values of α (0.1, 1, 2.2, 3, 4, 5, 6, 7, 9, 10, 14, and 20).

is in excellent agreement with results reported by Shankar,[29] who calculated that the height of a three-dimensional eddy structure in a cylindrical container of infinite depth is equal to $1.3995D$.

On the other hand, z_p/D is approaching to zero for values of α greater than seven, and this indicates that there is a minimum value of the jet flow beyond which the velocity profile at the jet exit is no longer influenced by the crossflow (SRD in velocity less than 0.1%). This seems to be confirmed by a simulation performed for $\alpha = 20$. In this case, $\mathrm{SRD}(z_p, \alpha)$ is less than 0.001 everywhere in the pipe.

These results suggest that, for a given α, a segment of the pipe of minimum length $z_p(\alpha)$ should be included in the computational domain to account correctly for the interaction between crossflow and pipe flow.

C. Influence of Coupling and Velocity Profile on Jet Penetration

Our main objective is to evaluate the influence of the boundary conditions used to model the velocity profile at the jet exit on the numerical simulation of the transverse jet. To the best of our knowledge, no study is available in the literature in which the impact of the choice of boundary condition on calculated jet penetration and spreading has been assessed. Therefore, we investigate the jet evolution for different values of α when 1) the jet emerges from a long, straight pipe and the coupling with the transverse flow is simulated, and when 2) the velocity profile is prescribed at the jet exit and the coupling with the transverse flow is neglected.

For the same values of α examined earlier, $\alpha = 2.2$, 4, and 7, we characterize the influence of the velocity profile at the jet exit and the coupling by comparing the flowfield generated in the two configurations 1 and 2. Figure 5 shows the isocontours of the axial velocity in the xz plane (pipe case, Figs. 5a–5c, corresponding to coupled, fully developed jet flow and no-pipe case; Figs. 5d–5f, corresponding to uncoupled, top-hat jet flow). The values of the isocontours of w/U_{jet} vary from 0.7 (solid line) to 1.1, with a step of 0.1. The jet shape is qualitatively similar in the two configurations, whereas large differences in the velocity magnitude profile are found. We observe that, for the same α, in the no-pipe case, 1) the maximum axial velocity is lower; 2) the gradient of the vertical velocity in the radial direction is larger; and 3) the gradient of the vertical velocity in the vertical direction is lower.

Following Moussa et al.,[12] to quantify these differences in the velocity profile, we define a jet-exit axial momentum as

$$M_z = \int_0^{D/2} 2\pi r \cdot w^2 \, \mathrm{d}r \tag{3}$$

The axial momentum M_z is larger in the pipe case than in the no-pipe case (3.7, 3.5, and 2.9% for $\alpha = 2.2$, 4, and 7, respectively). Similarly

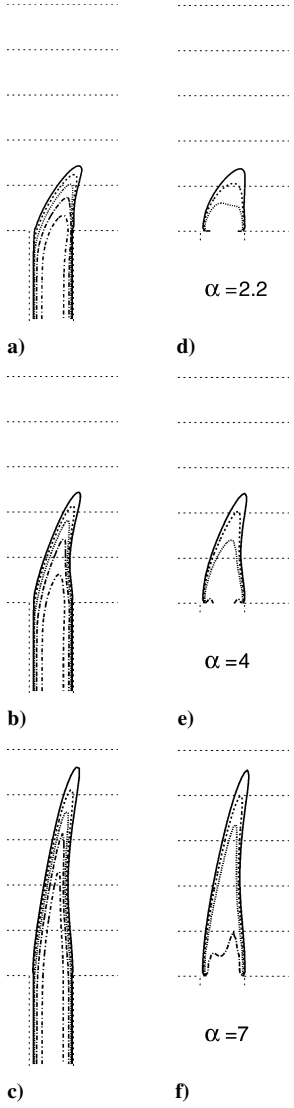

Fig. 5 Shape of jets issued from pipe and from hole in wall for α equal to a) and d) 2.2, b) and e) 4, and c) and f) 7.

to freejets, larger jet penetration into the crossflow is expected for velocity profiles characterized by larger momentum.

To quantify jet penetration, we calculated the jet axis for the different values of α examined. Figure 6 shows the jet axis for the two conditions; open and solid symbols correspond to pipe and no-pipe configurations, respectively. As expected, 1) the jet penetration increases for increasing values of α (Ref. 12); 2) for the same value of α, the penetration is larger in the no-pipe case; 3) the differences between jet axes, which are larger for smaller values of α, become negligible for α equal to 7. Point 2 seems to be in contradiction with observations made earlier because higher penetration is obtained in the no-pipe case, corresponding to lower maximum axial velocity and lower axial momentum. Nevertheless, similar observations have been reported by Moussa et al.[12] They explained differences observed in jet rise for a fluid issuing from a hole in the wall or from a pipe as a consequence of different entrainment of outer fluid and different momentum flux. This suggests that maximum axial velocity and axial momentum are insufficient to characterize jet behavior and some other quantities, that is, the rate of entrainment or the momentum flux may control the development of the jet shear layer and its evolution in the outer flow. In the no-pipe configuration, the shear-layer thickness at the jet exit is zero, and velocity gradients in the shear layer at the edge of the jet are stronger. This factor may contribute to the higher penetration of the jet in the no-pipe case,[11] which is presumably linked to a reduced centerline mean decay rate of velocity, already observed by Mi et al.[11] for freejets. As observed

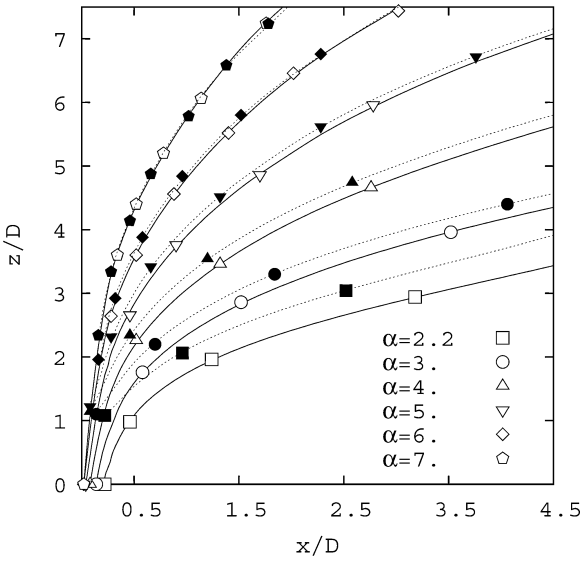

Fig. 6 Jet axis for α = 2.2, 3, 4, 5, 6, and 7: for pipe (open symbols) and no-pipe (solid symbols) configurations.

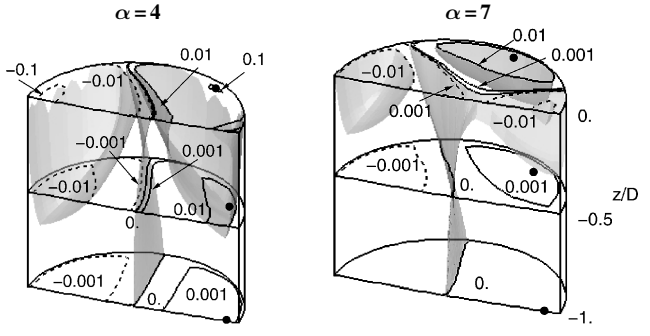

Fig. 7 Isocontours of $(w - w_{\text{pipe}})/U_{\text{jet}}$ at $z/D = -1, -0.5$, and 0 for α = 4 and 7 when α is obtained considering U_{jet} fixed and U_{cf} changing: ●, position of maximum velocity difference in cross section of pipe.

by Ashforth-Frost and Jambunathan[10] and Mi et al.,[11] in regard to freejets, these effects can also play a major role on the dynamics of the resulting large-scale convective structures of transverse jets, influencing both the deflection and spreading rate of the jet.

D. Effect of Unperturbed Crossflow Boundary Layer on the Extent of Coupling

As observed earlier, both jet-to-crossflow velocity ratio and unperturbed crossflow boundary-layer thickness contribute in determining transverse jet dynamics. Therefore, we performed a few test simulations (for $\alpha = 4$ and 7) to verify the effect of different crossflow velocities at the jet exit on the extent of the coupling inside the nozzle and on jet penetration. Results are shown in Figs. 7 and 8. Specifically, we compare the results obtained from simulations performed for $\alpha = 4$ and 7 when 1) U_{cf} is fixed (and equal to Shandorov's experiment) and $U_{\text{jet}} = \alpha \cdot U_{\text{cf}}$, or 2) U_{jet} is fixed (and equal to Shandorov's experiment) and $U_{\text{cf}} = U_{\text{jet}}/\alpha$.

Figure 7 presents the relative difference within the pipe between the axial velocity of the jet in crossflow and the freejet. Similarly to Fig. 3, we show the local velocity difference isosurfaces scaled by U_{jet}, that is, $(w_{\text{jcf}} - w_{\text{fj}})/U_{\text{jet}}$, calculated for $\alpha = 4$ and 7 and the corresponding isocontours at $z/D = -1.0$, -0.5, and 0.0 in case 2. Isocontours and isosurfaces are most similar to those shown in Fig. 3, indicating that the thickness of the unperturbed crossflow boundary layer at the jet exit has a negligible effect on the depth of crossflow interaction within the pipe. This seems to be confirmed by calculations made for z_p, shown as open circles in Fig. 4. The difference calculated in z_p/D for cases 1 and 2 is 0.02 for $\alpha = 4$ and 0.04 for $\alpha = 7$. Interestingly, larger variations are found for larger α.

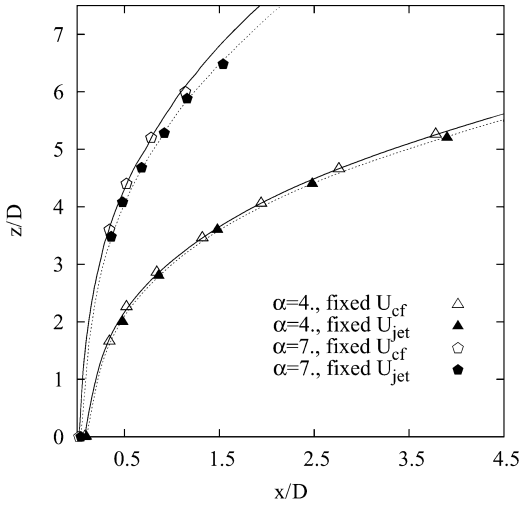

Fig. 8 Jet axis for $\alpha = 4$ and 7, comparison of axis penetration when same α is obtained: △ and ⬠, U_{cf} fixed and changing U_{jet} or ▲ and ⬟, U_{jet} fixed and changing U_{cf}.

Even though the unperturbed crossflow boundary-layer thickness at the jet exit has a negligible effect inside the pipe, it modifies the jet penetration. Figure 8 compares the jet axis calculated for $\alpha = 4$ and 7 in conditions 1 and 2. For both simulated values of α, the jet axis calculated for simulation 2 lies below the jet axis calculated for simulation 1. This difference is more evident for $\alpha = 7$ than for $\alpha = 4$. These results are in agreement with observations by Andreopoulos[18] and can be explained by considering how the unperturbed boundary-layer thickness changes in the different cases. Following Schlichting,[30] the boundary-layer thickness $\delta(x)$ grows proportionally to $(\nu x/U_{\text{cf}})^{0.5}$, where x indicates the distance from the crossflow inlet section, that is, the leading edge. In our simulations, $x = 5D$. In the simulations performed for increasing values of α when U_{jet} is fixed, U_{cf} is progressively reduced, increasing the value of δ at the jet orifice. We can argue that a larger unperturbed boundary-layer thickness leads to a stronger interaction between the jet and crossflow, which reduces jet penetration. Note that, for conditions examined in this work ($\alpha = 4$ and 7), the reduction of jet penetration measured $2D$ downstream the jet orifice is less than 5% for $\alpha = 7$.

IV. Conclusions

Dynamics and dispersion mechanisms of transverse jets are partially controlled by the coupling between the jet and the crossflow at the jet exit. This coupling is crucial to predict jet penetration and spreading rate correctly and yet is often neglected. We considered a pipe issuing the jet into the wind/water tunnel as a simplified model for a generic plenum/nozzle apparatus. We have characterized the time-averaged effect of the transverse stream on the flow within the pipe, 1) identifying the importance of accounting for the coupling between jet and crossflow and 2) considering the effect of different velocity profiles at the jet exit. We have demonstrated the importance of including a segment of pipe of appropriate length into the simulation of a transverse jet, also quantifying the minimum length required. We have evaluated the differences calculated in jet penetration when different boundary conditions are imposed to simulate the jet exit. Finally, we have characterized the effect of different crossflow velocities (and different unperturbed boundary-layer thickness) on the penetration of the jet. Results show that the coupling and a precise characterization of the velocity profile can be neglected only for velocity ratios greater than seven. This study may provide useful guidelines for future numerical investigations of the jet in crossflow.

Acknowledgments

Support from Centro Regionale di Assistenza Tecnica per le Aziende di Sedie e Mobili (UD, Italy) is gratefully acknowledged. This study was partially supported also by Regione Friuli Venezia

Giulia and by the Natural Sciences and Engineering Research Council of Canada under Grant RGPIN217169. We thank one of the anonymous reviewers for her/his insightful remarks, which helped us to improve the manuscript. One of the authors, L. C., thanks Ann R. Karagozian for enlightening discussions.

References

[1]Fric, T. F., and Roshko, A., "Vortical Structure in the Wake of a Transverse Jet," *Journal of Fluid Mechanics*, Vol. 279, 1994, pp. 1–47.

[2]Kelso, R. M., Lim, T. T., and Perry, A. E., "An Experimental Study of Round Jets in a Cross-Flow," *Journal of Fluid Mechanics*, Vol. 306, 1996, pp. 111–144.

[3]Yuan, L. L., Street, R. L., and Ferziger, J. H., "Large-Eddy Simulations of a Round Jet in Crossflow," *Journal of Fluid Mechanics*, Vol. 379, 1999, pp. 71–104.

[4]Rivero, A., Ferré, J. A., and Giralt, F., "Organized Motions in a Jet in Crossflow," *Journal of Fluid Mechanics*, Vol. 444, 2001, pp. 117–149.

[5]Cortelezzi, L., and Karagozian, A., "On the Formation of the Counter-Rotating Vortex Pair in Transverse Jets," *Journal of Fluid Mechanics*, Vol. 446, 2001, pp. 347–373.

[6]Mungal, M. G., and Lozano, A., "Some Observations of a Large, Burning Jet in Crossflow," *Experiments in Fluids*, Vol. 21, No. 4, 1996, pp. 264–267.

[7]Campolo, M., Salvetti, M. V., and Soldati, A., "Mechanisms for Microparticle Dispersion in a Jet in Crossflow," *AIChE Journal*, Vol. 51, No. 1, 2005, pp. 28–43.

[8]Karagozian, A. R., Cortelezzi, L., and Soldati, A. (eds.), *Manipulation and Control of Jets in Crossflow*, Springer-Verlag, Vienna, 2003, pp. 1–25.

[9]Beer, J. M., and Chigier, N. A., *Combustion Aerodynamics*, Applied Science, London, 1972.

[10]Ashforth-Frost, S., and Jambunathan, K., "Effect of Nozzle Geometry and Semiconfinement of the Potential Core of a Turbulent Axisymmetric Free Jet," *International Communications in Heat and Mass Transfer*, Vol. 23, No. 2, 1996, pp. 155–162.

[11]Mi, J., Nobes, D. S., and Nathan, G. J., "Influence of Jet Exit Conditions on the Passive Scalar Field of an Axisymmetric Free Jet," *Journal of Fluid Mechanics*, Vol. 432, 2001, pp. 91–125.

[12]Moussa, Z. M., Trischka, J. W., and Eskinazi, S., "The Near Field in the Mixing of a Round Jet With a Cross-Stream," *Journal of Fluid Mechanics*, Vol. 80, 1977, pp. 49–80.

[13]Andreopoulos, J., and Rodi, W., "Experimental Investigation of Jets in a Crossflow," *Journal of Fluid Mechanics*, Vol. 138, 1984, pp. 93–127.

[14]McCloskey, R. T., King, J. M., Cortelezzi, L., and Karagozian, A. R., "The Actively Controlled Jet in Crossflow," *Journal of Fluid Mechanics*, Vol. 452, 2002, pp. 325–335.

[15]Rudman, M., "Simulation of the Near Field of a Jet in a Cross Flow," *Experiments in Thermal and Fluid Science*, Vol. 12, No. 2, 1996, pp. 134–141.

[16]Hahn, S., and Choi, H., "Unsteady Simulation of Jets in a Cross Flow," *Journal of Computational Physics*, Vol. 134, No. 2, 1997, pp. 342–356.

[17]Hsu, A. T., He, G., and Guo, Y., "Unsteady Simulation of a Jet-in-Crossflow," *International Journal of Computational Fluid Dynamics*, Vol. 14, 2000, pp. 41–53.

[18]Andreopoulos, J., "On the Structure of Jets in a Crossflow," *Journal of Fluid Mechanics*, Vol. 157, 1985, pp. 163–197.

[19]Chochua, G., Shyy, W., Thakur, S., Brankovic, A., Lienau, J., Porter, L., and Lischinsky, D., "A Computational and Experimental Investigation of Turbulent Jet and Crossflow Interaction," *Numerical Heat Transfer*, Vol. 38, No. 6, 2000, pp. 557–572.

[20]Smith, S. H., and Mungal, M. G., "Mixing, Structure and Scaling of the Jet in Crossflow," *Journal of Fluid Mechanics*, Vol. 357, 1998, pp. 83–122.

[21]Abramovich, G., *The Theory of Turbulent Jets*, MIT Press, Cambridge, MA, 1963.

[22]Kuzo, D. M., "An Experimental Study of the Turbulent Transverse Jet," Ph.D. Dissertation, California Inst. of Technology, Pasadena, CA, 1995.

[23]Drikakis, D., "Bifurcation Phenomena in Incompressible Sudden Expansion Flows," *Physics of Fluids*, Vol. 9, No. 1, 1997, pp. 76–87.

[24]Patankar, S. V., and Spalding, D. B., "A Calculation Procedure for Heat, Mass and Momentum Transfer in Three Dimensional Parabolic Flows," *International Journal of Heat and Mass Transfer*, Vol. 15, 1972, pp. 1787–1806.

[25]Stuben, K., and Trottenberg, U., "Multigrid Methods: Fundamental Algorithms, Model Problem Analysis and Applications," *Multigrid Methods: Proceedings of Koln-Porz Conference on Multigrid Methods*, edited by W. Hackbusch and U. Trottenberg, Lecture Notes in Mathematics 960, Springer-Verlag, Berlin, 1982.

[26]Ajersch, P., Zhou, J. M., Ketler, S., Salcudean, M., and Gartshore, I. S., "Multiple Jets in a Crossflow: Detail Measurements and Numerical Simulations," *Journal of Turbomachinery*, Vol. 119, No. 2, 1997, pp. 330–342.

[27]Marchioli, C., Giusti, A., Salvetti, M. V., and Soldati, A., "Direct Numerical Simulation of Particle Wall Transfer and Deposition in Upward Turbulent Pipe Flow," *International Journal of Multiphase Flow*, Vol. 29, No. 6, 2003, pp. 1017–1038.

[28]Antonia, R. A., and Zhao, Q., "Effect of Initial Conditions on a Circular Jet," *Experiments in Fluids*, Vol. 31, No. 3, 2001, pp. 319–323.

[29]Shankar, P. N., "Three Dimensional Eddy Structure in a Cylindrical Container," *Journal of Fluid Mechanics*, Vol. 342, 1997, pp. 97–118.

[30]Schlichting, H., *Boundary Layer Theory*, McGraw–Hill, New York, 1979.

S. Mahalingam
Associate Editor